

Chapter 12

Land Degradation Assessment Using Geospatial Techniques



Arijit Barman, Nirmalendu Basak, Bhaskar Narjary, and Tarik Mitran

Contents

12.1	Introduction	423
12.2	Geographical Extent of Land Degradation: Global and Indian Perspective	425
12.3	Land Degradation Processes	427
12.3.1	Water Erosion	428
12.3.2	Wind Erosion	429
12.3.3	Chemical Degradation	429
12.3.4	Anthropogenic and Agricultural Activity	430
12.4	Causes of Land Degradation Process	431
12.5	Indicators of Land Degradation Assessment	432
12.6	Land Degradation Assessment Using RS and GIS Techniques	433
12.6.1	Aerial Image Processing	434
12.6.2	Satellite Image Processing	434
12.6.3	Ground-Based Sensing	441
12.6.4	Methodology of Land Degradation Mapping: Visual Interpretation and Digital Approaches	442
12.6.5	Assessing Spatial and Temporal Pattern of Salt-Affected Soils: A Case Study	444
12.7	Conclusions and Future Perspectives	446
	References	447

Abstract Land degradation is a thoughtful threat involved in reducing area and productivity of 13.4 billion ha in the global cultivable land. The genesis and distribution of different types of land degradation processes depend on climate, topography, vegetative cover, parent material (salty or acidic), and groundwater (saline, sodic, or heavy metals/metalloid). Above all, human-induced degradation of land has been exaggerated recently. These changes in land degradation can be

A. Barman (✉) · N. Basak · B. Narjary
ICAR-Central Soil Salinity Research Institute, Karnal, Haryana, India
e-mail: arijit.barman@icar.gov.in; nirmalendu.basak@icar.gov.in; bhaskar.narjary@icar.gov.in

T. Mitran
Soil and Land Resources Assessment Division, National Remote Sensing Centre, Department of Space, ISRO, Hyderabad, Telangana, India
e-mail: tarikmitran@nrsc.gov.in

monitored and assessed through geospatial techniques such as remote sensing (RS) and geographic information system (GIS) with fine spatial and spectral resolution imageries. The advanced techniques such as microwave, hyperspectral, and proximal ground-based sensor data with multivariate statistical algorithms have increased the efficiency of classification and mapping of degraded lands. The values of different parameters extracted from thematic map of the terrain, surface, hydrology, and spectral ratio indices of multispectral, hyperspectral images are used as an input parameter for the generation of a digital soil map. The digital soil map with seasonal/temporal variation (possible with fine temporal resolution) conveys detailed information regarding the study of changes, characterization, causes, protection, and reclamation of the land degradation processes. The method of real-time monitoring and assessment of land degradation using RS/GIS techniques is cost-effective, fast, and accurate and indicates land/resource management quickly to secure the food, water, and environmental security. This chapter summarizes the comprehensive understanding of the extent, type, cause of land degradation processes, and indicators of land degradation as well as assessment and monitoring of such through advanced remote sensing techniques.

Keywords Degraded soils · Ground-based sensor · Geographic information system · Hyperspectral · Multispectral · Synthetic aperture radar · Temporal variation

Abbreviation

ANN	Artificial Neural Networks
ASTER	Advanced Spaceborne Thermal Emission and Reflection Radiometer
AVHRR	Advanced Very High Resolution Radiometer
BART	Bayesian Additive Regression Trees
CT	Classification Tree
DEM	Digital Elevation Model
ESP	Exchangeable Sodium Percentage
ETM+	Enhanced Thematic Mapper Plus
GBM	Gradient Boosting Machines
GIS	Geographic Information System
HRS	Hyperspectral Remote Sensing
IRS	Indian Remote Sensing
LDN	Land Degradation Neutrality
LISS	Linear Imaging Self Scanning
MODIS	Moderate Resolution Imaging Spectroradiometer
MSS	Multispectral Scanner System
NDSI	Normalized Difference Salinity Index
NDVI	Normalized Difference Vegetation Index
NDWI	Normalized Difference Water Index
NIR	Near Infrared
PCR	Principal Component Regression

PLSR	Partial Least Squares Regression
RF	Random Forest
RS	Remote Sensing
RT	Regression Tree
SAR	Synthetic Aperture Radar
SAVI	Soil-Adjusted Vegetation Index
SI	Salinity Index
SPAD	Soil Plant Analysis Development
SPOT	Système Pour l'Observation de la Terre
SVM	Support Vector Machine
SVR	Support Vector Regression
SWIR	Shortwave Infrared
TDR	Time-Domain Reflectometry
TM	Thematic Mapper
UNCCD	United Nations Convention to Combat Desertification
VI	Vegetation Index
VNIR	Visible and Near Infrared

12.1 Introduction

Land degradation is a challenge for the existence, prosperity, and future of any civilization. Currently, several types of land degradation are major threats for the developing countries for declining productivity of soil, water, pastureland, agricultural, and economic growth further arising of conflict at a regional level and question of security of livelihood (Reddy 2003). Agricultural production is deleteriously affected due to inappropriate land care strategies in maximum portions of the world (FAO 2005; Lambin and Meyfroidt 2011; Lambin et al. 2013). Sometimes, direct land degradation may appear in expanding the area under desertification in semi-arid and arid climatic region, frequent and intense drought occurrence, extreme types of water, and wind erosion promote a severe amount topsoil loss and flooding leads to a reduction of soil productivity, alterations of soil properties, biodiversity deterioration and encourages the loss of soil organic carbon (Foley et al. 2005; Gibbs et al. 2010; Lambin and Meyfroidt 2011). The main physical agents of land degradation are water, wind, expansion of the desert and flood, etc. Among these wind erosion, high wind velocity and intense heat carry the top fertile soils from one area to other sites, and soil nutrients are lost carried out to certain distance, and subsoil gets exposed and soil loss with productivity due to lost away of fertile soil. The secondary land degradation arises mainly due to the rapid development of irrigation infrastructure without the optimum implementation of irrigation practices, and drainage measures have caused a rise in the water table, and consequent widespread waterlogging and salinization in several arid and semi-arid regions in the world (Tyagi 1998). Agricultural intensification arises stress on soil resources,

the decline in soil quality, and overexploitation of groundwater. Such intensification increases the cost of cultivation, decrease/deposition of nutrient content, the decline in organic carbon of soil, distortion of soil structural, the addition of salts and toxic chemicals, and decline in soil resilience and resistance (Lal and Stewart 1990; Basak et al. 2014; Bhattacharyya et al. 2015). Land productivity from all aspects has been reduced by human intervention during land preparation, overexploitation of vegetation, and overgrazing, leading to soil quality deterioration (UNEP 1992; Holm et al. 2003; Kniivila 2004). The extent of land degradation varies from region to region and rapidly changes with time. There is a problem with the availability of clear information on the extent of land degradation, neither worldwide nor a particular country (FAO 2008; Bindraban et al. 2012; Mitran et al. 2018). Monitoring of land degradation depends on visual and digital analysis of an image, ground-truthing of soil, water, the pattern of the river, water bodies, land surface, land cover, natural vegetation, crops, temperature, rainfall pattern and shift, the presence of salts, toxic pollutants and determination of the source of contaminants and pollutants. Therefore, to cope with the adverse effect of land degradation, undertaking RS and GIS applications is vital for rapid and real-time estimation and assessment of the extent, type, and nature of degraded lands. Assessment, monitoring, and rehabilitation of degraded lands are the options to minimize the gap between supply and demand of our daily needs and improve agricultural productivity, strengthening the economy of agrarian countries. The digital soil maps with seasonal/time variation (possible with fine temporal resolution) give detailed information regarding changes, characterization, causes, protection, and reclamation of the land degradation process. Land degradation is a thoughtful threat which involved in reducing area and productivity of 13.4 billion ha in the global cultivable land. Space Applications Centre of India (SAC) (2016) reported that out of the total geographic area (TGA), 96.4 Mha (29.3%) areas come under the land degradation process in India. Change analysis after 10 years reported that 1.95 Mha lands have been reclaimed and around half million ha land reduced its severity level from high to medium, whereas 0.75 Mha land converted to high severity level from low in India. The genesis and distribution of different types of land degradation processes depend on climate, topography, vegetative cover, parent material (salty or acidic), and groundwater (saline, sodic, or heavy metals/metalloids). Above all, human-induced degradation of land has been exaggerated recently. These changes in land degradation can be monitored and assessed using different techniques of RS and GIS with fine spatial- and spectral-resolution imagery. The advanced techniques such as microwave, hyperspectral, and proximal ground-based sensor data such as multispectral, hyperspectral, microwave, and ground-based sensor, viz. EM38, time-domain reflectometry (TDR), spectroradiometer, ground-penetrating radar (GPR), resistivity meter, soil plant analysis development (SPAD), green shaker, and chlorophyll meter, with multivariate statistical algorithm (principal component regression (PCR), partial least-squares regression (PLSR), random forest (RF), support vector machine (SVM), etc.), have increased the efficiency of classification and mapping of degraded lands. The values of different parameters, extracted from thematic map of the terrain, surface and hydrology, and spectral ratio indices [normalized difference vegetation

index (NDVI), soil-adjusted vegetation index (SAVI), normalized difference water index (NDWI), etc.] of multispectral, hyperspectral images, are used as an input parameter for the generation of a digital soil map. The method of real-time monitoring and assessment of land degradation using RS/GIS techniques is cost-effective, fast, and accurate and indicates land/resources management quickly to secure the food, water, and environmental security. Land degradation is a thoughtful threat which involved in reducing area and productivity of 13.4 billion ha in the global cultivable land. The genesis and distribution of different types of land degradation processes depend on climate, topography, vegetative cover, parent material (salty or acidic), and groundwater (saline, sodic, or heavy metals). Above all, human-induced degradation of land has been exaggerated recently. These changes in land degradation can be monitored and assessed through geospatial techniques such as RS and GIS with fine spatial- and spectral-resolution imageries. The advanced techniques such as microwave, hyperspectral, and proximal ground-based sensor data with multivariate statistical algorithm have increased the efficiency of classification and mapping of degraded lands. The values of different parameters, extracted from thematic map of the terrain, surface, hydrology, and spectral ratio indices of multispectral, hyperspectral images, are used as an input parameter for the generation of a digital soil map. This digital soil map with seasonal/temporal variation gives detailed information regarding changes, characterization, causes, protection, and reclamation of the land degradation processes. This chapter summarizes the comprehensive understanding of the extent, type, cause of land degradation processes, and indicators of land degradation as well as assessment and monitoring of such through advanced remote sensing techniques.

12.2 Geographical Extent of Land Degradation: Global and Indian Perspective

The estimated global total degraded land area was varied from 0.99 to >6.0 billion ha (UNCCD 2017). These huge discrepancies among researchers are mainly due to their approaches and lack of cohesiveness. In a worldwide, mainly, three methodologies have been followed to estimate degraded lands, i.e. expert view, RS observation, and biophysical models. Global-estimated land degradation by these approaches is presented in Table 12.1.

According to the Global Assessment of Human-Induced Soil Degradation (Bridges and Oldeman 1999), globally, ~15% of the land was found to be degraded. Among the various agents, soil erosion, nutrient loss, salinity, soil physical problems, and chemical contamination degrade 83, 4, 4, 4, and 1% of the land, respectively. In South Asia, 43% of the agricultural land was degraded. Among this strongly degraded land was 31.0 Mha, and moderately degraded land was 63.0 Mha. The severely affected country was Iran (94% of agricultural land under

Table 12.1 Percent of degraded lands based on three methodologies

Area	Expert opinion			Satellite observation	Biophysical models
	Dregne and Chou (1992)	GLASOD	FAO TerraSTAT	GLADA	Cai et al. (2011)
Africa	29.12	26.40	19.90	24.09	13.32
Asia	37.36	37.25	40.73	33.28	49.45
Australia and Pacific	10.47	0.49	5.99	8.61	1.31
Europe	2.62	12.99	6.56	2.37	10.49
North America	11.94	11.51	12.96	17.12	9.69
South America	8.52	11.43	13.86	14.53	15.74

Modified, Gibbs and Salmon (2015)

GLASOD Global Assessment of Soil Degradation, FAO Food and Agriculture Organization, GLADA Global Assessment of Land Degradation and Improvement

degradation), and the least affected was Bhutan (10%). Only because of land degradation South Asian countries are losing US\$10 billion annually.

Land degradation assessment using satellite remote sensing helped to present precisely the spatial distribution of global degraded lands. However, the main limitation of this method is to separate saline and naturally low productive areas from those human degraded lands. However, it was observed that soil degradation information derived from RS imageries in slightly and moderately degraded areas was less accurate. This limits the perspective of RS for land degradation assessment specifically in the low to moderately degraded areas. Based on NDVI imageries on land productivity, GLADA estimated a falling inclination of net primary productivity (NPP) over 21% of global land area, ranging from tropical Africa, Southeast Asia, Australia, and North America. In the biophysical approach of land degradation assessment, cropping suitability of land was combined with productivity. Based on this approach, Cai et al. (2011) reported that globally, 1.0 billion ha of lands (approximation) were affected by various types of land degradation and of which China and India contained nearly 490.0 Mha of degraded lands.

Unlike the world database, in India, a systematic approach has been followed for estimating degraded land. According to the latest land degradation assessment (SAC 2016) in 2013, 96.4 million hectares of land area affected by land degradation, representing 29.3% of India's total land area. Around 24.0% of the total geographic area was degraded mainly in the arid and semi-arid regions of India (Rajasthan, Jharkhand, Maharashtra, Gujarat, etc.). Although 1.95 Mha of land was reclaimed within 2003–2005 to 2011–2013, surprisingly, it was observed that during the same period, 3.63 Mha of productive land had undergone degradation. From 2003 to 2013, severe land degradation (11.03 to 4.34%) was observed in the states of Delhi, Nagaland, Tripura, Mizoram, and Himachal Pradesh, whereas maximum land reclamation (0.11 to 1.27%) was noticed in Odisha, Rajasthan, Telangana, and Uttar Pradesh. Among all the land degradation processes, water erosion contributed the

Table 12.2 Process wise land degradation status during 2003 and 2013 in India (percent of total area under desertification, modified, SAC 2016)

Process of land degradation	Degraded land area (%)	
	2003	2013
Deforestation	29.92	30.39
Water erosion	37.67	37.45
Wind erosion	19.41	18.91
Salinity	4.24	3.81
Waterlogging	0.63	0.67
Frost shattering	3.29	3.46
Mass movement	0.89	0.96
Manmade	0.39	0.43
Barren/rocky	1.99	1.96
Settlement	1.57	1.95

most (37.0%), followed by deforestation (30%) and wind erosion (19%) (Table 12.2). During 2003–2013, an area under desertification increased from 81.5 to 82.6 Mha. Wind erosion is the main significant process of desertification in the arid region, while deforestation and water erosion are the main process of degradation in the regions of semi-arid and dry subhumid.

In recent estimates (SAC 2016) of salt-affected land, only 3.67 Mha areas were affected by salinity and alkalinity. But these estimates have a huge deviation from the earlier estimates (6.73 Mha) done by National Remote Sensing Centre (NRSC), Central Soil Salinity Research Institute (CSSRI), and National Bureau of Soil Survey and Land Use Planning (NBSSLUP). They have used LANDSAT satellite data corresponding to 1996 along with soil chemical analysis data and estimated the total salt-affected area of 6.73 Mha and out of which saline soil cover 2.9 Mha and sodic soil cover 3.7 Mha in India (Mandal et al. 2010). This large difference in totality as well as on the spatial distribution of salt-affected degraded lands illustrates the scalability of the problem and the necessity of accurate data and techniques for estimation salt-affected areas.

12.3 Land Degradation Processes

The project of GLASOD (Oldeman et al. 1991) distinguishes four types of soil degradation around the world such as water erosion, wind erosion, chemical degradation (salinization/alkalization, acidification), and physical degradation (glacial, waterlogging), but nowadays, anthropogenic factors become more dominant due to pressure of burgeoning population. In India, NRSC (2010) had used a 13-fold major category to generate wasteland (degraded land) map at 1:250,000 and

1:50,000 scale using visual and digital remote sensing techniques) under National Wastelands Monitoring Project. These 13-fold major categories are as follows:

1. Gullied and/or ravinous (eroded) lands
2. Undulating uplands with or without scrub
3. Marshy and water stagnated land
4. Coastal or inland salinity/alkalinity affected lands
5. Shifting cultivation area
6. Degraded informed forest land
7. Pastures/grazing land degradation
8. Degraded non-forest plantation area
9. Sandy areas in the desert or coastal region
10. Wasteland in the industrial/mining area
11. Barren/sheet/stony rocky area
12. Sloppy (steep) areas
13. Snow/glacial areas

These 13-fold categories can be broadly grouped as water and wind erosion, waterlogging, salinization/alkalization, acidification, glacial, anthropogenic, and others.

12.3.1 Water Erosion

Worldwide water erosion is an important hazard, and annually, ~24 billion tonnes of top fertile soil is washed away (FAO 2011; Meena et al. 2018). This soil erosion also aggravated a loss of 1100 Mt. C into the atmosphere and conjointly erosion-induced transportation loss of 300–800 Mt. C to the ocean through soil loss (Lal 2011). Besides organic C loss, water erosion also results in losses of inherent and applied nutrients, the soil compacted as top fertile soil eroded out, loss in soil biodiversity, and chances of contamination with heavy metals and pesticides. Water erosion negatively affects crop productivity. It has an important threat to the security of food, livelihood, and environment in a country. In India, around 13.4 Mt. (~205.32 billion rupees) of annual productions are lost due to water erosion (Sharda et al. 2010). The climatic, physiographic, and parent material characteristics show a 32% water erosion registered for the southern plateau region, while north India claimed 68% registered water erosion (NAAS 2017). In north India, the Brahmaputra, the Ganges, and the Indus, rivers which flow the northern Himalayan region, jointly contribute half of the total gross erosion in India.

12.3.2 Wind Erosion

Wind erosion is the process of movement of soil particles by strong wind regime which cross over the critical velocity for beginning the movement of soil particles (Samra et al. 2012). The topsoil erosion disturbs the soil air composition, soil temperature and water status, microbial respiration, and carbon storage in soils. In the region of semi-arid and arid, nearly devoid of native or planted vegetation with high wind velocity tends to wind erosion. The single grained sandy soils are most prone to this erosion. The finer soil particle and externally applied soil nutrients are carried out to a certain distance, and subsoil get exposed and soil loss with productivity due to blown away of fertile soil. The Sahelian Africa (Sterk 2003), northern China (Yan et al. 2005), and North-western Thar Desert of India are severely affected by wind erosion.

12.3.3 Chemical Degradation

Soils that need unusual management are collectively known as chemically degraded soil or problem soils. These types of soils are characterized by the excess or deficiency of some characteristics parameters and making it barren or less productive soil. These soils are affected by different degrees of soil degradation problems.

12.3.3.1 Salinization/Alkalization

The higher content of electrolytes (cations and anions) causes the problem of salinity. The presence of salts causes the high osmotic potential results in plants and native soil microbes start experiencing severe water stress due to the physiological unavailability of water. Further, antagonism relation between electrolytes (Cl^- and H_2PO_4^-), (Cl^- and NO_3^-), (Cl^- and SO_4^{2-}), and (Na^+ and K^+) affects the normal nutrition of the plant, whereas high pH_s and alkalinity ($\text{pH}_s > 8.5$) and exchangeable sodium percent ($> 15\%$) create the problem of the low permeability of water and air entry in soil due to dispersion of aggregates and clay particles. The hard crust on the surface delays seedling emergence. The toxic concentration of alkaline anion (HCO_3^- and CO_3^{2-}) causes a deficiency of N, Zn, and Fe (Rai et al. 2020; Basak et al. 2020).

12.3.3.2 Acidification

Soil having pH ranges from 4.5 to 6.5 categorized as acid soil. The deficiency of P, Ca, and Mg and excess of Al^{3+} , Fe^{3+} , and Mn^{3+} cause root injury and soil limited soil biological activity.

12.3.3.3 Physical Degradation

The unfavourable soil physical conditions make soil underproductive. The major soil physical constrains are soil compaction due to mechanical impedance, crust formation, hardening and sealing of topsoil, low water retention and highly permeable soil, shallow soils, and slowly permeable soil.

12.3.3.4 Waterlogged Soil

Water table rises to such an extent that the root zone becomes saturated with water. Impair in aeration results in poor crop growth and limited nutrient uptake. The nitrification process is badly affected.

12.3.4 Anthropogenic and Agricultural Activity

The populous country (like India and China) achieves security for food production by an intensification of agriculture. This intensification and associated food security are accomplished with a huge challenge and a serious deterioration and degradation of soil and land quality. Burgeoning population drastically shrinks the land availability (land-human ratio) in India with land availability decline 0.34 ha in 1961–52 to 0.14 ha in 2012–2013 and expected it will decline further. Therefore, it is inevitable to raise in more pressure for finite soil resources and prone to degradation for perceive agricultural productivity, sustaining economic growth (IPES-Food 2019). High fertilizer consumption for agriculture intensification increases its negative fates, a possibility for its indiscriminate use also enhanced with attendant loss of efficiency and imbalances in rates of the fertilizing nutrients particularly NPK. Such imbalances in fertilization eventually cause deterioration in the health of soils and the environment simultaneously. Symptoms of such deterioration of soil health are captured by different researchers computing soil quality index under various fertilization treatments and cropping systems in a large number of long-term fertility experiments in diverse agroclimatic areas (Basak and Mandal 2019).

The important key visual interpretation feature of several types of land degradation depends on colour, texture, pattern, size, shape, association, etc. Identification of different land degradation process depends on different types of land degradation.

Table 12.3 Keys of visual image analysis for different land degradation

Process	Colour	Shape	Texture	Pattern
Water erosion	Slightly brighter/brighter grey to dark grey than surrounding land	Irregular	Smooth/medium to coarse	Contiguous/discrete patches to contiguous patches
Wind erosion	Light grey/yellow to pink mottles	Irregular/regular	Smooth/medium to coarse	Contiguous/discrete patches/mottling
Waterlogging	dark or shaded blue/grey	Irregular/regular	Smooth	Discrete/contiguous patches
Salinization/alkalization	Light grey/greyish white to white/dull white	Irregular	Smooth	Discrete patches
Acidification	Green/black shades	Irregular	Smooth-medium	Contiguous/discrete patches/mottled
Anthropogenic (industrial effluent, mining, brick factory)	Shaded/dull white, grey, blue to yellow, red, black	Irregular/Regular	Smooth-medium	Contiguous/discrete/Isolated patches

Modified, Ravishankar and Sreenivas (2010)

The false colour composite (FCC) image helps to identify the different types of land degradation processes. Some of the important visual interpretation features of land degradation process have been presented in Table 12.3.

12.4 Causes of Land Degradation Process

The causes of land degradation are directly/indirectly linked to human activities. The pressure of the population in a rural and urban area with the development of the economy pressurizes the change of land use, leading to the function and productivity degradation of an ecosystem (Cherlet et al. 2018). Removal of soil covers by the means of overgrazing, deforestation and deterioration of soil health by agricultural activity overdose of fertilizer, and nutrient mining for supporting the increasing demand of national are the core reasons for land degradation. Man-made soil deterioration rate has been projected based on changes in local population densities (both human and animal) and/or in relation to mechanization, agricultural expansion, fertilizer use, etc. during 10 years. The reason for land degradation differs from country to country (Table 12.4). Deforestation followed by agriculture is the dominant cause of degradation in Asia and South America, whereas, in Africa and South America, it is overgrazing and agriculture, respectively. Australia and New Zealand of the Oceania continent are the main contributors to overgrazing. Overutilization by woodcutting for fuel purposes is very high in lower developing continents, while this scenario is absent in developed continents, where other causes of degradation became prominent (Table 12.4).

Table 12.4 Sources of human-induced land degradation (percent of total human-induced degraded land; Modified, Oldeman 1992)

Area	Deforestation	Overutilization	Overgrazing	Agricultural practices	Mechanization
Asia	15.17	2.34	10.03	10.38	0.05
Europe	4.27	0.05	2.54	3.26	1.07
Africa	3.41	3.21	12.37	6.16	–
North America	0.20	–	1.48	3.21	–
Central America	0.71	0.56	0.46	1.42	–
South America	5.09	0.61	3.46	3.26	–
Oceania	0.61	–	4.22	0.41	–
World	29.47	6.77	34.55	28.09	1.12

Gao and Liu (2010) reported that overgrazing, intensive cultivation, unnecessary reclamation of grassland for farming, and deforestation leads to the worsened degradation situation. They reported that land degraded area increased from 2400 to 4214 km² due to soil salinization, waterlogging, and desertification. A different agricultural activity like deforestation, overgrazing, excessive irrigation, groundwater withdrawal, intensive tillage operation with heavy agriculture machinery, crop residue burning and low return of organic input, impaired irrigation, drainage, and water management, monoculture and faulty crop rotation, and misuse of pesticide further aggravated the degradation (Bhattacharyya et al. 2015).

12.5 Indicators of Land Degradation Assessment

Identification of potential indicators of land degradation followed by empirical verification with ground-truthing and remote sensing data are used to measure and monitor spatial and seasonal variability of degraded land. The most important indicators are:

- Sparse vegetation/increased bare ground
- Increased soil looseness
- Reduction of soil organic matter
- The non-uniform rainfall distribution pattern
- High concentration of salts in soil surface
- Water stagnation on the soil surface
- Reduction of rain use efficiency (annual sum NDVI/annual rainfall)
- Reduction of energy use efficiency (annual sum NDVI/annual accrued temperature)

Most of these indicators directly or indirectly linked with the influence of vegetation which varies with the season, crop, and degree of maturity of the vegetation, soil and climate, and the kind of vegetative material, namely, roots, plant tops, and plant residues. Residue from vegetation protects the surface soil from raindrop impact and recovers the soil structure and organic carbon. Soil erosion can be reduced by control tillage and residue management practices. The major efforts of vegetation in reducing erosion are as follows:

- Surface sealing and runoff are reduced by the interception of rainfall by reducing the raindrop energy.
- Decreased surface velocity retards erosion and nutrient.
- Vegetation cover serves as a physical limit of soil displacement.
- Soil physical properties like porosity, structure, and aggregation are improved by root and crop residue.
- Improve soil biological activity.
- Water stagnation on the soil surface is reduced by plant transpiration and favour for the agroforestry system which reduces runoff and improves the soil storage capacity.
- Vegetation cover checks the evaporation and breaks the capillary rise of water; as a result, salt accumulation is reduced on the surface soil.

Besides vegetation cover, other indicators like inherent soil properties, slope, topographic position, volume, intensity and frequency characteristics of rain, and wind speed influence the degree of degradation.

12.6 Land Degradation Assessment Using RS and GIS Techniques

Degraded land in arid and semiarid regions creates a severe problem. Several researchers (FAO 2005; Lambin and Meyfroidt 2011; Lambin et al. 2013; Gelfand et al. 2013) reported that in many parts of the world, agricultural lands are shrinking and not enough to satisfy the demand of our daily need. Land scarcity becomes more vulnerable under the pressure of population growth especially, in the south-eastern countryside of Asia. In this scenario, degraded lands minimize the land scarcity problem by meeting the demand for food. However, regular monitoring and assessment of these lands in a spatiotemporal scale is a very difficult task. Many different approaches have been adopted by different researchers to monitor its type, extent, degree, rate, and causes; these can be grouped as (1) expert opinion during the survey and used to quantify the area and mapped; (2) biophysical modelling based on auxiliary parameters that indicate the crop productivity, which can be used as a proxy for assessment of degraded land; (3) abandonment of agricultural lands due to some economic, political, and low productive issue—these lands converted to a wasteland. All of these approaches take more time, capital, and labour; and (4) the

satellite-based approach comes to frontline due to the advancement of the satellite, software, and a new algorithm for estimating the area of degraded land and also can be assessed the cause of area extension. But the problem of delineation of degraded land using advanced different RS and GIS techniques has been overcome efficiently and very useful for monitoring purposes (Khan et al. 2005). The different features on the earth's surface can be identified using different RS data (Metternicht and Zinck 2003).

12.6.1 Aerial Image Processing

Colour/or tone, texture, pattern, association, and size of the vegetative canopy on aerial photographs and satellite images help directly or indirectly to detect the type of soil degradation. Among aerial and satellite images, the aerial image is the old technique of RS, and even today, it is used intensively for detailed study. To monitor the land degradation (salt-affected lands and waterlogged lands) from a small distance, (fine) resolution imaging/non-imaging sensor is mounted on drone with GPS to scan at a fixed time and space resolution and capture detailed information about degraded land. This aerial image is used to confirm the data interpretation along with RS images and served as supplement image (Haseena et al. 2013). Salt-affected soil surface is generally appeared as smoother and discrete patches over normal soil surfaces and gives high reflectance value in VNIR (visible and near-infrared) region (Dehni and Lounis 2012; Srivastava et al. 2017). But in waste or degraded land, the reflection is reduced in the VNIR region (Mandal 2019). However, the aerial photograph will be most useful in conjunction with other ground- and satellite-based RS techniques.

12.6.2 Satellite Image Processing

Land degradation differs from space to space and also with seasons which can be characterized by spatial, spectral, and temporal characteristics of different surface features (Metternicht and Zinck 2008). Defining land degradation and mapping criteria become more difficult when both surfaces, as well as subsurface variability, are considered. Notably, RS and GIS techniques with ground-based sensors are fetching popularize over conventional techniques for its fast assessment and estimation of land degradation for monitoring and mapping purposes. Both passive/active RS sensors are classified as multispectral, hyperspectral, and microwave sensors. Their amalgamation for assessment and prediction of degraded land has defined an extraordinary ability to monitor and map.

12.6.2.1 Multispectral Imagery

Integrated approach (Douaoui et al. 2006; Farifteh et al. 2006a, b; Eldeiry and Garcia 2008) of multispectral sensors (Landsat MSS, TM, ETM+, SPOT-XS, MODIS, Sentinel, Terra-ASTER, IRS-LISS-III and IV, IKONOS, Quick Bird, Hyperion, and World Vision satellite images) with ancillary information like terrain model data, spatial model data, geography survey data, and field information can increase the accuracy of degraded soil mapping (Setia et al. 2013; Rawat et al. 2018). Nowadays, multispectral advanced sensors capture images with fine (<1.0 m) spatial resolution, whereas coarse spatial with a high-spectral-resolution image can be fused with pan band, which has a fine spatial resolution; in this way, both spatial and spectral resolution of any image can be improved and subsequently become easy to update the information of slight to severe degree of degradation at fine scale in a very economical mode.

There was a 40% increase in salt-affected soils and waterlogged areas observed in Punjab within 5 years using IRS imageries under a project funded by the World Bank (Sethi et al. 2006). GIS platform with RS techniques was utilized for incorporating both non-spatial and spatial attributes, which were recorded from different sources like proximal sensing instrument, traditional laboratory analysis, and other sources to generate the spatiotemporal database and quantification of problem soil-related parameters through multivariate statistical modelling (Singh et al. 2010; Sethi et al. 2014). Digital image processing with visual interpretation and capturing of the spectral signature of salt-affected soils, waterlogged soil, vegetation, crop and sandy soils on multispectral FCC imagery with reference of NDVI (NIR-R/NIR + R), VI (NIR/R), etc. spectral index map are used to discriminate normal and stressed crops. Image classification techniques like maximum likelihood, random forest, and principal component classification with advance PCR, PLSR, and ANN algorithm and black box model (classification tree, regression tree, decision tree, etc.) have been used and optimized for monitoring and mapping of degraded soil (Metternicht and Zinck 2003; Dwivedi et al. 2008).

Waterlogged and salt-affected soils are mainly governed by groundwater quality and its depth. But to monitor the hydrogeological parameter, using RS imagery is very difficult. However, Sander (2007) predicted the depth and availability of water table through lineament analysis on RS imagery along with DEM image analysis using surface and hydrology tools of GIS. Currently, the temporal resolution of the satellite has been improved which helps to monitor the waterlogged status at different seasons. Techniques of RS and GIS become very handy to inaccessible areas within a short time and explore and evaluate the groundwater resources (Chowdhury et al. 2003). Hydrological with RS data had significantly used to explore aquifer geometry, details, and groundwater quality (Jha et al. 2007). Dubey and Sharma (2002) used a factor analytical model to establish a programming system to decide on the groundwater pollution potential with the help of RS, GIS, and auxiliary data. Satellite imagery and ancillary data have used in a GIS-based groundwater prediction model which enabled the prediction of the risk of

salinization by the prediction of groundwater level in the region of Murray Valley Irrigation Region of New South Wales, Australia (Lamble and Fraser 2002).

12.6.2.2 Hyperspectral Imagery

Most broadband data mainly multispectral data, derived from satellite-like Sentinel, AVHRR, IRS, SPOT, Landsat, etc., quantify the reflected radiation at a wide spectral band from surface features. Hyperspectral imagery (narrowband data) capture the reflected radiation at a sequence of 1.0 nm spectral bands. That's why one pixel of the hyperspectral image can supply huge information regarding any surface characteristics due to its high spectral resolution at a 1.0 nm interval, despite 30.0 m spatial resolution (Hyperion). A number of the spectral bands do not prove a sensor as a hyperspectral sensor. The main characteristic of a hyperspectral sensor is that it should be narrow (<10.0 nm) and produce contiguous spectral information. Spectra of soil, vegetation, and mineral have unique absorption drop at a different wavelength (Fig. 12.1a). Absorption peak shifted to higher wavelength with the increase of moisture content (Fig. 12.1b) and reflectance values in same soil are reduced with the increase of volumetric moisture content (Das et al. 2015; Fabre et al. 2015). These unique characteristics of spectra help to identify and quantify different properties of a certain material. Hyperspectral data/images can identify the different field crop canopy, in marginally and severely degraded areas, whereas multispectral images classify different vegetative growth and salinity intensity based on different spectral indices, and mapping of salt-affected soils is prepared maximum based on poor vegetative growth.

12.6.2.2.1 Spectral Libraries

Problem soil measurement using optical sensing (e.g. VNIR, SWIR) involves the fine-tuning of spectra for a degraded soil-related parameter using different multivariate statistical models. Existing spectral libraries (ESLs) and site-specific developed

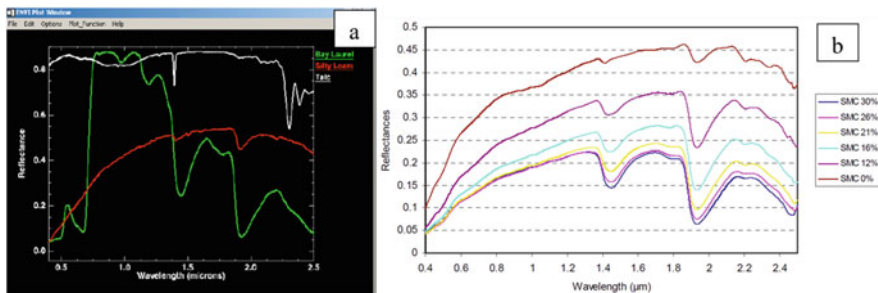


Fig. 12.1 Different spectra recorded by a spectroradiometer (a) for a vegetative cover, soil, talc mineral; (b) for soil with different moisture content. (Adopted, Fabre et al. 2015)

spectral libraries based on local soil samples (LSLs) are used for model fine-tuning (Shepherd and Walsh 2002; Viscarra Rossel and Webster 2012; Stevens et al. 2013). Nowadays, during the purchase of spectroradiometer, these ESL is supplied with instrumental software, which can be directly used for the prediction of different parameters without any analysis cost, whereas laboratory analysis cost is involved for LSL to develop an accurate (unbiased) local spectral model (Guerrero et al. 2014; Clairotte et al. 2016). Many researchers (Shepherd and Walsh 2002; Brown et al. 2006; Viscarra Rossel et al. 2016) reported that large capital is required to develop a regional-, country-, and global-level soil spectral library; that's why the cost is involved to utilize these developed spectral model for the calibration of the local spectral model. These developed spectral libraries reduce the laboratory analysis cost, time, and labour and make popularize the soil spectroscopy. In India, full-range (350.0–2500.0 nm) soil spectral library was prepared by Saxena et al. (2005) based on collected soil samples from different agroecological zones of the country. Similarly, Das et al. (2015) reported unique spectral characteristics of different soil orders of aridisols, inceptisols, alfisols, vertisols, and laterite soil across India. Vertisols have less reflectance value, whereas inceptisols have high reflectance value due to less clay content. Curcio et al. (2013) reported the all measured reflectance with average values for each soil groups. The soil texture varied from clay to clay loam, loam to sandy loam, and clay to silty clay loam for Pietranera, Dirillo, and Bompensiere soil of Sicily, Italy.

12.6.2.2 Methodology of Salt-Affected Soil Characterization and Mapping using HRS

Planning of salt-affected/problem soil mapping is a very difficult task due to the complexity of salt composition and its development process (salinization) along with seasonal and spatial variability. Identification of severely affected salt-affected soils using RS imagery is very easy for high reflectance value, whereas mixed reflectance value is recorded in the case of slight and moderately salt-affected soils for its association with soil, water, and crop canopy cover. New advanced methodology for salt-affected soil mapping and characterization was developed by CSSRI using multispectral, hyperspectral, proximal sensing for ground truth and different linear, non-linear, and black-box modelling of spectra for quantification of parameters. More than 90% of spatial variability of salt-affected soil parameters such as EC_e , saturated extract Cl^- , CO_3^{2-} , HCO_3^- , and Na^+ ($me\ L^{-1}$) can be predicted by hyperspectral modelling. Prominent absorption drops of 1.4, 1.9, and 2.2 μm were found in salt-affected soils of Haryana. Absorption drops at 1.9 μm shifted to higher waveband with the increase of salt concentration. The proposed methodology was found useful for delineating salt-affected soils from the space platform (Fig. 12.2).

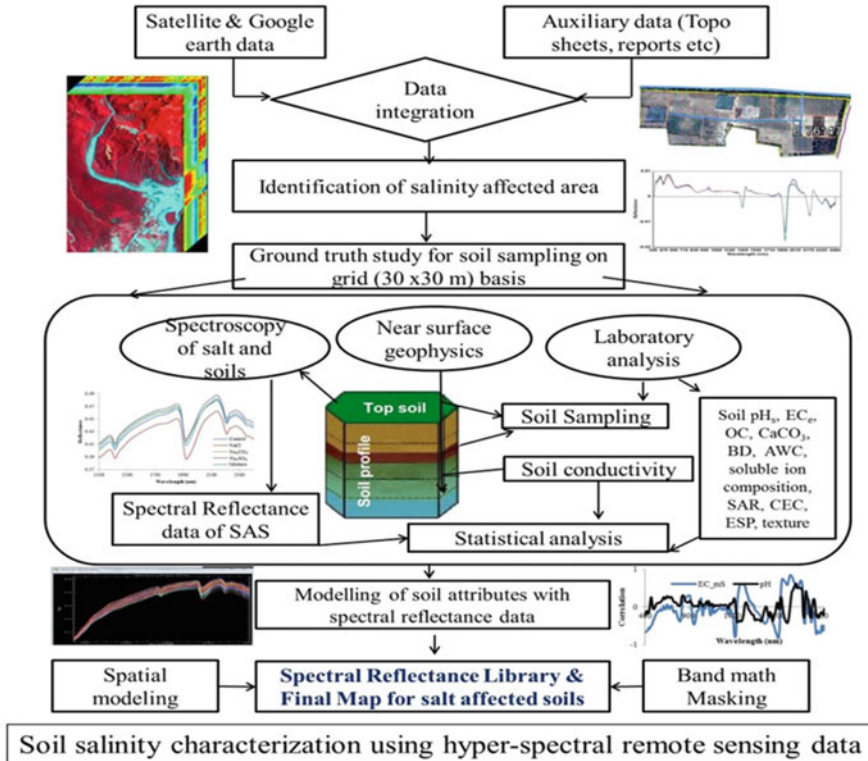


Fig. 12.2 Methodology for characterizing SAS using spectral data. (Adopted, Barman et al. 2017)

12.6.2.2.3 Prediction of Soil Attributes Based on Reflectance Data

Developed spectral models (Shepherd and Walsh 2002; Farifteh et al. 2004, 2006a, b, 2007, 2008; Wang et al. 2012; Mitran et al. 2015; Srivastava et al. 2017) by several workers using soil reflectance values and soil attributes were effectively used to predict different soil parameters. The multivariate spectral model has a huge potential to distinguish the type of land degradation in a precise region (Leone and Sommer 2000). Hyperspectral techniques with multi-temporal images solve the problem of similarity among salt-affected soil, sandy soil, and settlement (Lu et al. 2005; Farifteh et al. 2007). Representative waveband needs to be collected from mixed spectral tones of soil and crop cover to reduce errors in the NIR, red, and green bands, used for FCC image during classification (Rao et al. 1995; Metternicht and Zinck 2003; Farifteh et al. 2006a, b, 2008). Distinctive spectral reflectance in the VNIR region is reduced by hydrated evaporative minerals in salt-affected soils (Farifteh et al. 2008). A significant absorption drop was found at 505, 920, 1415, 1915, and 2205 nm. But there was a difference within the spectra of pure salt and

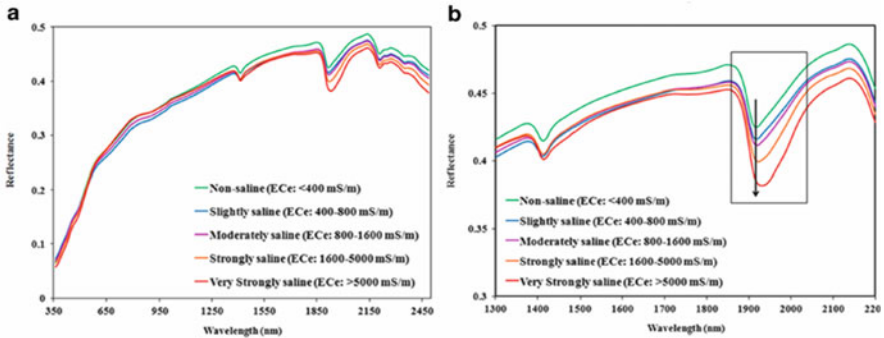


Fig. 12.3 Soil spectra with different salinity classes based on EC_e (dS m^{-1}) in the optical region (a) and shifting of absorption drop to higher wavelength with increase of salt concentration (b). (Adopted, Srivastava et al. 2017)

mixed salt with soil and/or associated with other minerals. In general, identification of degraded lands on an RS image faces the following problems:

- Absence of crust
- Mixing of degraded soil signature with others like sand and settlements
- Mixing of soil and vegetation cover
- Presence of soil moisture

Therefore, indirect mapping of degraded lands based on the vegetative spectral signature, affected by problem soil, increases the accuracy of mapping. Taylor and Dehaan (2000) reported that the decreasing trend of the reflection curve was observed in the NIR region (800–1300 nm). Different types of vegetation like vegetation under stress, narrow or broad leaves, cereal or legume, etc. can be studied using fine spectral resolution (Dehaan and Taylor 2001). High reflectance in the visible region over the NIR region of stressed vegetation (Weiss et al. 2001) helps to identify the different soil-related stress (Tilley et al. 2007). Hyperspectral images, i.e. Hyperion data (Weng et al. 2008), HyMAP (Dehaan and Taylor 2003), ASTER (Melendez-Pastor et al. 2010), and different indices of problem soil such as normalized difference vegetation index (NDVI), salinity index (SI), normalized difference salinity index (NDSI) (Huete 1998; Huete et al. 2003), and soil-adjusted vegetation index (SAVI) using Landsat imagery (Bannari et al. 2008; Jabbar and Chen 2008; Odeh and Onus 2008) can identify the different category of SAS. Kumar et al. (2015) showed a significant coefficient of determination ($R^2 > 0.75$) with soil salinity-related parameter (EC_e , SAR, and ESP). In India, NBSS&LUP (2006) developed a national soil spectral library, including problem soils, and this library can be used to increase the precision of degraded soil map. Srivastava et al. (2017) showed the effect of different salt concentrations based on EC_e (mS m^{-1}) in the optical region on soil spectral signature (Fig. 12.3a). The variation of absorption peak (on first derivative spectra) was more prominent at 1.4, 1.9, and 2.2 μm . There was a shifting of

absorption drop to a higher wavelength with an increase of salt concentration at 1.9 μm (Fig. 12.3b).

12.6.2.3 Microwave Sensors in Land Degradation Assessment

Microwave RS, i.e. synthetic aperture radar (SAR) data, has huge potential in the delineation of saline/sodic and waterlogged soils despite cloudy weather conditions (Metternicht 1998; Bell et al. 2001; Metternicht and Zinck 2003). The information from the SAR image has huge potential in the mapping of environmental change. The microwave RS (backscattering) works based on the principle of dielectric constant-polarization (Engman 1991), the roughness of features, wavelength or frequency (Evans et al. 1992), slope, and orientation, i.e. look angle. The results of small perturbation model (SPM), physical optics (PO), semi-empirical polarimetric model (SEPM), Dubois model (DM), and other algorithms were compared with soil texture, salinity, frequency, moisture content, and vegetation canopy parameters to estimate imaginary part of the dielectric constant of soil. The real part of the radar backscattering model is associated with moisture content, whereas the imaginary part is responsible for salt concentration. These soil properties depend on the backscattering coefficient which depends on the dielectric constant of soil, and this dielectric property depends on free water, bound water, air, and soil solids. Soil salinity mainly depends on free water content. Low-frequency (L-band or high-wavelength) microwave RS (active/passive) is best for the mapping of surface salt-affected soil (Dongryeol 2003). The sensitivity of imaginary soil dielectric constant proportionately correlates with salinity and moisture (Sreenivas et al. 1995). Jain (2011) measured the dielectric constant by inversed co-polarized techniques from SAR images and reported that this technique identifies soil salinity (EC) in Unnao district of Uttar Pradesh, India. The derived radar attributes have also potential in the mapping of degraded soil in an irrigated condition of Chubut, Argentina (Del Valle et al. 2009). There is a possibility to differentiate the salinity from sodicity using L waveband under wet soil regimes. Long wavelength of microwave RS can penetrate soil and vegetation. The soil penetration depends on profile moisture, but long wavelength, i.e. P (30.0–100.0 cm wavelength) and L bands (15.0–30.0 cm wavelength), has high energy to penetrate the feature over C band (3.8–7.5 cm wavelength) (Bell et al. 2001; Lasne et al. 2008). These SAR images are validated using radiometers (ground-based microwave) for the study of degraded soils. Chakraborty et al. (2013) enlisted the area of applicability of Indian radar satellite (RISAT-1) with HH, VV, HV, and VH polarizations, and these are vegetation, crop monitoring, flood mapping, salinity monitoring, degraded soil mapping, forestry study, soil moisture study, estimation of rice productivity, geology study, sea ice, and coastal monitoring.

12.6.3 *Ground-Based Sensing*

Data from space-based satellite images can be validated by ground-based imaging/non-imaging data. These ground-based advanced electronic sensors and other proximal devices such as electromagnetic/electrical probes, time-domain reflectometry—TDR (emissivity), resistivity tool, salinity and moisture sensors (electrochemical), chlorophyll meter (optical), and ground-penetrating radar with GPS devices are used to record data from less height of the feature surface at the field for the mapping and monitoring of degraded status. Ground-penetrating radar and TDR are indirectly linked with soil surface/underground moisture and salt concentration. These handy tools are very cost-effective (Aldabaa et al. 2015) and can be mapped and/or in situ monitor based on an empirical site-specific model of infiltration and profile moisture (French and Binley 2004; Jayawickreme et al. 2008), EC, and resistivity model (Slater and Sandberg 2000; Kemna et al. 2002) with less time and capital (Hamed et al. 2003; Robinson et al. 2003). The ground-penetrating radar (for groundwater survey) can sense the little variation in salt and water movement at <30.0 m soil depth (Ludwig et al. 2011); however, this tool shows its difficulty in soil with $EC > 4.0 \text{ dS m}^{-1}$ and $SAR > 13.0$ due to high attenuation of backscattering. Goldshleger et al. (2010) generated a 3D map of land degradation in cropland using hyperspectral RS, frequency-domain electromagnetic induction (FDEM), and ground-based radar data. Sethi et al. (2014) estimated soil and plant properties using IRS and ground data to manage the problem soils of Haryana, India. Multi-spectral image with DEM gives more information regarding paleo-drainage patterns, sunken area, playas, and catchment areas which are very useful to estimate the water accumulation, recharging potential during heavy rainfall (Kwarteng 2002). Guo et al. (2015) reported that backscattering coefficient from HH polarization of ALOS/PALSAR radar imagery and apparent electrical conductivity (EC_a) value of EM38 sensor were imported to ArcGIS platform to perform the spatial model with a geostatistical tool to know the variability of moisture and salt concentration of soil, respectively, in reclaimed coastal of south Hangzhou Gulf. Traditional laboratory determination of salinity and sodicity are costly and laborious and requires intensive time to get desired information. Electromagnetic (EM) induction techniques are nowadays widely used as an alternative tool for collecting information on soil properties relevant to salinity and sodicity. Recently, in India, geophysical EM induction techniques were used to characterize soil salinity and their extent and represent soil salinity three-dimensionally (Narjary et al. 2017, 2019; Koganti et al. 2018). But lots of research is required to standardize and development of models to get its effective application for degradation land mapping and monitoring.

12.6.4 Methodology of Land Degradation Mapping: Visual Interpretation and Digital Approaches

Multispectral imageries of three different crop growing periods (*kharif*, *rabi*, and *zaid*) can be used as input to identify the seasonal variation of land degradation (Fig. 12.4) using an on-screen digitization technique (SAC 2016; NRSC 2020). These satellite data are processed in image processing software with the help of image enhancement, visual interpretation, spectral ratio, and ancillary information/legacy data as thematic maps, existing LULC, wasteland map, and other printed material. Satellite image processing and interpretation are very important for the identification of ground-truth sample collection. Different types of land degradation can be visually identified based on colour/tone, texture, pattern, size, shape, and association (explained in Sect 12.3.4). Collected soil samples are analysed for pH_s, EC_e texture, organic carbon, exchangeable cation and anion, CaCO₃ percentage, etc. These are used to develop the final land degradation map after the validation and accuracy assessment.

However, various digital approaches have also been adopted for qualitative and quantitative assessment of degraded soils by various researcher across the world

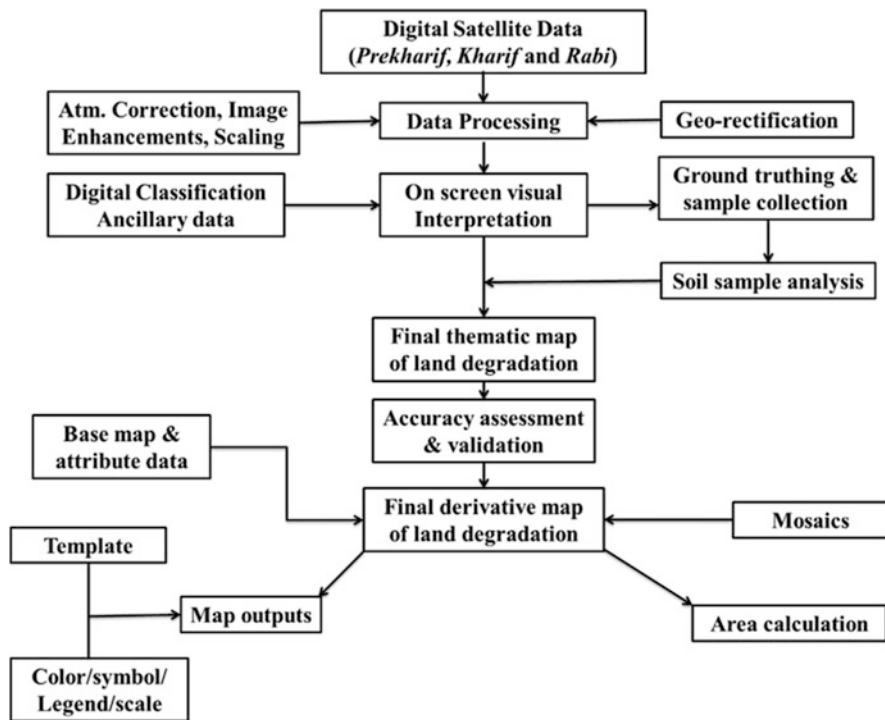


Fig. 12.4 Methodology of land degradation mapping. (Modified, Ravishankar and Sreenivas 2010)

Table 12.5 Methodology and remote sensing data used in different studies for land degradation assessment

Land degradation processes	Study area	Method	Data used	References
All land degradation processes	India	On-screen visual interpretation along with soil sample analysis	IRS AWiFS (1:500 K)	SAC (2016)
All land degradation processes	India	On-screen visual interpretation along with soil sample analysis	LISS-III (1:50 K)	NRSC (2015, 2020)
Soil salinity Mapping	Bhavnagar, Gujarat	Spectral angle mapper algorithm	Hyperion data	Mitran et al. (2015)
Soil moisture and salinity stress	Dharmapuri, India	Microwave and multi-spectral model	Radar Imaging Satellite and Landsat data	Periasamy and Shanmugam (2017)
Surface waterlogging	Rohtak, India	Thresholding of NDWI for optical image and Sigma0 for SAR images	Sentinel 2 MSS images and Sentinel 1A SAR images	Kaushik et al. (2018)
Dynamics of waterlogged area	Bangladesh	Random forest classification based on training pixel	Landsat imageries (Time series)	Islam et al. (2018)
Saline soil map	SE Spain	Matched filtering (MF) and mixture-tuned MF	ASTER Images	Melendez-Pastor et al. (2010)
Hydro saline land degradation	Faisalabad, Pakistan	Salinity indices and digital image processing	IRS-1B	Khan et al. (2005)
Salinity stress	Hakim Farabi Farming in Iran	Hyperspectral vegetation indices	Hyperion image	Hamzeh et al. (2013)
Wind erosion hazard mapping	Laghouat region (Algeria)	Fuzzy logic approach	Landsat 8 OLI images	Saadoud et al. (2018)
Soil wind erosion	Inner Mongolia, China	Improved AHP and a weighted summation method	AVHRR and MODIS NDVI	Zhou et al. (2015)
Acid sludge concentration in soil	Balikpapan, East Kalimantan (Indonesian)	NDVI method	Landsat images	Haryani et al. (2017)
Acid mine drainage map	Mpumalanga Province of South Africa	Spectral signatures of jarosite and haematite	Landsat 8	Sakala et al. (2017)
Trace metal content in Soils	New York	Correlation analysis (surrogate)	ASD data	Wu et al. (2010)

(continued)

Table 12.5 (continued)

Land degradation processes	Study area	Method	Data used	References
Soil loss by water erosion	Australia	Factors of RUSLE estimation to model soil loss by water erosion	SRTM and MODIS data	Teng et al. (2016)
Deforestation detection	Viti Levu Island, Fiji	MulTiFuse approach for detecting deforestation	Landsat and SAR time series	Reiche et al. (2015)

(Table. 12.5). They have used multispectral, hyperspectral, and microwave satellite datasets to map degraded soil through different modelling techniques. A number of researchers have used various hyperspectral based indices and algorithm to assess and map soil salinity at regional scale (Melendez-Pastor et al. 2010; Hamzeh et al. 2013; Mitran et al. 2015). Saadoud et al. (2018) generated wind erosion hazard map at Laghouat region in Algeria using Landsat 8 OLI data using the fuzzy logic approach. Teng et al. (2016) assessed soil loss by water erosion in Australia using SRTM and MODIS data using an universal soil loss equation. Dynamics of water-logged area was mapped by Islam et al. (2018) using Landsat time-series datasets through random forest classification technique. Kaushik et al. (2018) were used NDWI thresholding method on optical image and SAR images of Sentinel 1 and 2 to map surface waterlogging in parts of Rohtak, Haryana, India.

12.6.5 Assessing Spatial and Temporal Pattern of Salt-Affected Soils: A Case Study

12.6.5.1 Study area

An experiment was conducted by CSSRI in the Nain experimental farm of Panipat, Haryana (between 29°18'37.93"N longitude to 29°19'20.86"N latitude and 76°47'08.62"N longitude and 76°48'21.79"E longitude) states of India to study the changing pattern of salinity/sodicity through RS and GIS using field-based observation.

12.6.5.2 Data and Methodology

The high temporal resolution of any satellite images helps to monitor the extent and pattern of degraded land over a time period in a specific region. Hence, different seasonal satellite datasets of years 2011–2012 and 2017–2018 (here, IRS LISS III and Landsat satellite imageries) of a year were collected and corrected by the removal of the effects of sun elevation angle, atmospheric influences, and normalization of radiometric differences for comparing the land degradation. The satellite

data was used to identify the salt-affected soils at the study site through visual interpretation technique. After the identification of the area, the soil samples were collected. The sampling time and weather condition have a great impact on the increment of area. Hence, the surface (0–15 cm) soil samples were collected during April–May during 2011–2012 and 2017–2018, and that time salt has been accumulated to the surface due to high evaporative demand during hot dry weather condition.

The soil samples were analysed for pH_s and EC_e using standard protocols. The spatial interpolation technique, i.e. ordinary kriging, was used to create spatial soil pH_s and EC_e map of the experimental site for 2011–12 and 2017–18. Both the maps were used to assess the changes in soil salinity and sodicity over 6 year period.

12.6.5.3 Salient Findings

The spatial pattern of EC_e and pH_s of the study site is presented in Fig. 12.5. Results of the study show that the extent of soil salinity increased by 8.3 and 15.8% (Table 12.6) over 6 years period in moderate (EC_e 8.0–30.0 $dS\ m^{-1}$) and strong ($EC_e > 30.0\ dS\ m^{-1}$) salinity region, respectively, whereas, the extent of pH_s increased by 28.9 and 20.3% (Table 12.6) over 6 years period, in the region where pH_s ranges from 8.2–8.5 and > 8.5 , respectively.

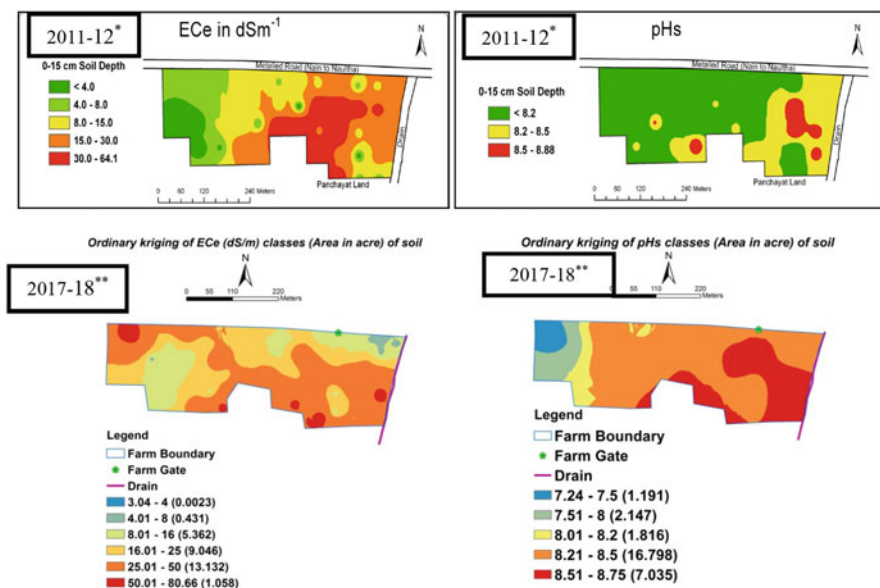


Fig. 12.5 Changes of salinity/sodicity after 6 years. (Adopted, *Mandal et al. 2013 and **CSSRI 2018)

Table 12.6 Changes of surface soil salinity and sodicity over 6 years

Soil properties	Range in property	Percent of the total area (2011–12*)	Percent of the total area (2017–18)	$\Delta_6\%$ area
pH _s	<8.2	67	17.8	49.2
	8.2–8.5	29	57.9	(+) 28.9
	>8.5	4	24.3	(+) 20.3
EC _e (dS m ⁻¹)	<4.0	8.7	0.01	8.69
	4.0 to 8.0	16.9	1.49	15.41
	8.0 to 15.0	25.4	15.4	10
	15.0–30.0	31.2	49.5	(+) 18.3
	>30	17.8	33.6	(+) 15.8

Adopted, CSSRI (2018) and *Mandal et al. (2013)

12.7 Conclusions and Future Perspectives

Remotely sensed data become more efficient when it combines with numerical modelling. Predictive models to estimate degraded soil-related parameters are empirical and site-specific in nature and have limited applicability beyond the area of development, but for qualitative assessment of degraded soil for mapping, monitoring and some management practices can be done using multispectral imagery, and its accuracy can be improved by using hyperspectral, radar, and ground-based sensor. So, there is a need to develop methodologies for rapid detection and mapping of salt-affected soil by integrating satellite RS with ground-based proximal sensors. Ground truthing is a must for removing the confusion of mixed pixel or signatures and also used for accuracy assessment in the mapping of degraded soil. All spectral, GPS, and ground-based sensor data are imported to a GIS platform which provides an efficient handling and management system for handling large and complex databases for land degradation assessment studies. Predicting warmer temperatures, change of rainfall distribution pattern and intensity, rising sea level, etc. leads to a change in the extent of degraded land. Therefore, monitor and assessment of degraded soil of any country becomes a flagship program after a minimum of 3–5 years interval due to a change of climatic scenarios. With the growing interest on high-resolution satellite imagery data applicability, rapid assessment of soil salinity, sodicity, acidity, waterlogged, and wasteland through visual and digital models that are encouraging as it assists in real-time precise monitoring of degraded soil over the spatiotemporal context and also helps in the collection of spectral signature, facilitating the farmers to manage more effectively and efficiently based on the mobile-based decision support system in regional language. As a new step of the digital era, digital soil mapping of a country gives the detailed information of each point of the map and stored spectral library in Web-GIS server help to retrieve any information or parameters related to degraded soils. The collaboration of different sensors (e.g. optical, microwave, and

thermal sensors) and platforms (e.g. ground-based, air-based, and space-based sensing) improves the accuracy and reproducibility of degraded soil map in time. In 2015, United Nations Convention to Combat Desertification (UNCCD) has developed Land Degradation Neutrality (LDN) programme in collaboration with multiple international partners (over 120 countries) and committed to setting LDN targets, and out of these, 80 countries have already set their target. The LDN target follows the Sustainable Development Goal (SDG) target 15.3 which states to achieve a land degradation-neutral world by combating desertification and restoration of degraded land and soil by 2030. In this scenario India sets its target to restore degraded lands from 21 Mha to 26 Mha, by 2030 (Press Information Bureau, Ministry of Environment, Forest and Climate Change, GOI, 2019). Geospatial techniques can play a meaningful role in support to achieve LDN target through the qualitative and quantitative assessment of land resources which are necessary to the ecosystem functions and services and enhance food security and production by the reclamation and restoration process.

Acknowledgements The authors are thankful to PME (No.-Research Article/83/2019) and Director, ICAR-Central Soil Salinity Research Institute, Karnal, Haryana, and Head of Soil and Crop Management for sustain encouragement for writing the chapter. The authors also gratefully acknowledge Dr s. Madhurama Sethi, Rajeev Srivastava and AK Mandal for their constructive support.

References

- Aldabaa AAA, Weindorf DC, Chakraborty S, Sharma A, Li B (2015) Combination of proximal and remote sensing methods for rapid soil salinity quantification. *Geoderma* 239–240:34–46
- Bannari A, Guedona AM, El-Hartib A, Cherkaouic FZ, El-Ghmari A (2008) Characterization of slightly and moderately saline and sodic soils in irrigated agricultural land using simulated data of advanced land imaging (EO-1) sensor. *Commun Soil Sci Plant Anal* 39(19–20):2795–2811
- Barman A, Mandal AK, Srivastava R, Yadav RK, Sharma PC (2017) Soil salinity characterization using hyper-spectral remote sensing data. *ICAR News* 23(4):11–12
- Basak N, Mandal B (2019) Soil quality management through carbon farming under intensive agriculture systems. *Indian J Fertil* 14(12):54–64
- Basak N, Datta A, Mandal A, Ghoshal SK, Mandal B (2014) Improving quality and resilience of soils under rice-based cropping systems. *Indian Farming* 64(1):10–13
- Basak N, Barman A, Sundha P, Rai AK (2020) Recent trends in soil salinity appraisal and management. In: Rakshit A, Ghosh S, Chakraborty S, Philip V, Datta A (eds) *Soil analysis: recent trends and applications*. Springer, Singapore, pp 143–162
- Bell D, Menges C, Ahmad W, Van Zyl JJ (2001) The application of dielectric retrieval algorithms for mapping soil salinity in a tropical coastal environment using airborne polarimetric SAR. *Remote Sens Environ* 75:375–384
- Bhattacharyya R, Ghosh BN, Mishra PK, Mandal B, Rao CS, Sarkar D, Das K, Anil KS, Lalitha M, Hati KM, Franzluebbers AJ (2015) Soil degradation in India: challenges and potential solutions. *Sustainability* 7:3528–3570
- Bindraban PS, van der Velde M, Ye L, van den Berg M, Materechera S, Kiba DI, Tamene L, Ragnarsdóttir KV, Jongschaap R, Hoogmoed M, Hoogmoed W (2012) Assessing the impact of soil degradation on food production. *Curr Opin Environ Sustain* 4(5):478–488

- Bridges EM, Oldeman LR (1999) Global assessment of human induced soil degradation. *Arid Soil Res Rehabil* 13(4):319–325
- Brown DJ, Shepherd KD, Walsh MG, Dewayne MM, Reinsch TG (2006) Global soil characterization with VNIR diffuse reflectance spectroscopy. *Geoderma* 132(3–4):273–290
- Cai X, Zhang X, Wang D (2011) Land availability for biofuel production. *Environ Sci Technol* 45(1):334–339
- Chakraborty M, Panigrahy S, Rajawat AS, Kumar R, Murthy TVR, Haldar D, Chakraborty A, Kumar T, Rode S, Kumar H, Mahapatra M, Kundu S (2013) Initial results using RISAT-1 C-band SAR data. *Curr Sci* 104(4):491–501
- Cherlet M, Hutchinson C, Reynolds J, Hill J, Sommer S, von Maltitz G (2018) World atlas of desertification. Publication office of the European Union, Luxembourg
- Chowdhury A, Jha MK, Machiwal D (2003) Application of remote sensing and GIS in groundwater studies: an overview. In: *Proceedings of the International Conference on Water & Environment (WE-2003), Ground Water Pollution, December 15–18, MP, India*, pp 39–50
- Clairotte M, Grinand C, Kouakoua E, Thebault A, Saby NPA, Bernoux M, Barthes BG (2016) National calibration of soil organic carbon concentration using diffuse infrared reflectance spectroscopy. *Geoderma* 276:41–52
- CSSRI (2018) Annual Report 2017–18. Central Soil Salinity Research Institute, Karnal, India
- Curcio D, Ciraolo G, D'Asaro F, Minacapilli M (2013) Prediction of soil texture distributions using VNIR-SWIR reflectance spectroscopy. *Procedia Environ Sci* 19(494):494–503
- Das BS, Sarathjith MC, Santra P, Sahoo RN, Srivastava R, Routray A, Ray SS (2015) Hyperspectral remote sensing: opportunities, status and challenges for rapid soil assessment in India. *Curr Sci* 10:860–868
- Dehaan RL, Taylor GR (2001) Mapping irrigation-induced salinity with hyperspectral imagery. In: *Proceedings of the international geoscience and remote sensing symposium, IGARSS '01, IEEE International*, pp 293–295
- Dehaan R, Taylor GR (2003) Image-derived spectral end members as indicators of salinization. *Int J Remote Sens* 24(4):775–794
- Dehni A, Lounis M (2012) Remote sensing techniques for salt affected soil mapping: application to the Oran region of Algeria. *Procedia Eng* 33:188–198
- Del Valle HF, Blanco PD, Sione W, Rostagno CM, Elissalde N (2009) Assessment of salt affected soils using multisensory radar data—a case study from Northeastern Patagonia (Argentina). In: *Metternicht G, Zinck JA (eds) Remote sensing of soil salinization: impact on land management*. CRC Press, Boca Raton, pp 155–173
- Dongryeol R (2003) Microwave emission of high-saline soils. Lecture at Merit Melbourne Engineering Research Institute, Melbourne
- Douaoui AEK, Nicolas H, Walter C (2006) Detecting salinity hazards within a semiarid context by means of combining soil and remote-sensing data. *Geoderma* 134(1–2):217–230
- Dregne HE, Chou NT (1992) Global desertification dimensions and costs. *Degradation & Restoration of Arid Lands*:73–92
- Dubey OP, Sharma DC (2002) Integrated remote sensing and factor analytic GIS model for evaluating groundwater pollution potential
- Dwivedi RS, Kothapalli RV, Singh AN (2008) Generation of farm level information on salt-affected soils using IKONOS-II multispectral data. In: *Metternicht G, Zinck JA (eds) Remote sensing of soil salinization: impact on land management*. CRC Press, Taylor & Francis, Boca Raton
- Eldery A, Garcia LA (2008) Detecting soil salinity in alfalfa fields using spatial modeling and remote sensing. *Soil Sci Soc Am J* 72(1):201–211
- Engman ET (1991) Applications of microwave remote sensing of soil moisture for water resources and agriculture. *Remote Sens Environ* 35:213–226
- Evans DL, Farr TG, Van Zyl JJ (1992) Estimates of surface roughness derived from synthetic aperture radar (SAR) data. *IEEE Trans Geosci Remote Sens* 30(2):382–389

- Fabre S, Briottet X, Lesaignoux A (2015) Estimation of soil moisture content from the spectral reflectance of bare soils in the 0.4–2.5 μm domain. *Sensors* 15(2):3262–3281
- FAO (2005) The state of food insecurity in the world 2005: Eradicating world hunger e key to achieving the millennium development goals
- FAO (2011) The State of the World's Land and Water Resources for Food and Agriculture (SOLAW): managing systems at risk. FAO, Rome, p 50
- Farifteh J, Bouma A, Van Der Meijde M (2004) A new approach in the detection of salt affected soils; integrating surface and subsurface measurements. Poster presented at “Near surface 2004”, 10th EAGE European Meeting of Environmental and Engineering Geophysics, Utrecht, The Netherlands
- Farifteh J, Van der Meer F, Carranza EJM (2006a) Similarity measures for spectral discrimination of salt-affected soils. *Int J Remote Sens* 28:5273–5293
- Farifteh J, Farshada A, George RJ (2006b) Assessing salt-affected soils using remote sensing, solute modelling, and geophysics. *Geoderma* 130:191–206
- Farifteh J, Van Der Meer F, Atzberger C, Carranza EJM (2007) Quantitative analysis of salt affected soil reflectance spectra: a comparison of two adaptive methods (PLSR and ANN). *Remote Sens Environ* 110:59–78
- Farifteh J, Van Der Meer F, Van Der Meijde M, Atzberger C (2008) Spectral characteristics of salt-affected soils: a laboratory experiment. *Geoderma* 145:196–206
- Foley JA, DeFries R, Asner GP, Barford C, Bonan G, Carpenter SR, Chapin FS, Coe MT, Daily GC, Gibbs HK, Helkowski JH (2005) Global consequences of land use. *Science* 309(5734):570–574
- Food and Agriculture Organization (2008) The state of food and agriculture, Biofuels: Prospects, risks and opportunities, pp 1–138
- French H, Binley A (2004) Snowmelt infiltration: monitoring temporal and spatial variability using time-lapse electrical resistivity. *J Hydrol* 297:174–186
- Gao J, Liu Y (2010) Determination of land degradation causes in Tongyu County, Northeast China via land cover change detection. *Int J Appl Earth Obs Geoinform* 12(1):9–16
- Gelfand I, Sahajpal R, Zhang X, Izaurralde RC, Gross KL, Robertson GP (2013) Sustainable bioenergy production from marginal lands in the US Midwest. *Nature* 493(7433):514–517
- Gibbs HK, Salmon JM (2015) Mapping the world's degraded lands. *Appl Geogr* 57:12–21
- Gibbs HK, Ruesch AS, Achard F, Clayton MK, Holmgren P, Ramankutty N, Foley JA (2010) Tropical forests were the primary sources of new agricultural land in the 1980s and 1990s. *Proc Natl Acad Sci* 107(38):16732–16737
- Goldshleger N, Ben-Dor E, Lugassi R, Eshel G (2010) Soil degradation monitoring by remote sensing: examples with three degradation processes. *Soil Sci Soc Am J* 74:1433–1445
- Guerrero C, Stenberg B, Wetterlind J, Viscarra Rossel RA, Maestre FT, Mouazen AM, Zornoza R, Ruiz-Sinoga JD, Kuang B (2014) Assessment of soil organic carbon at local scale with spiked NIR calibrations: effects of selection and extra weighting on the spiking subset. *Eur J Soil Sci* 65:248–263
- Guo Y, Shi Z, Huang J, Zhou L, Zhou Y, Wang L (2015) Characterization of field scale soil variability using remotely and proximally sensed data and response surface method. *Stoch Environ Res Risk Assess*, Springer, Berlin/Heidelberg
- Hamed Y, Persson M, Berndtsson R (2003) Soil solution electrical conductivity measurements using different dielectric techniques. *Soil Sci Soc Am J* 67:1071–1078
- Hamzeh S, Naseri AA, Alavipanah SK, Mojaradi B, Bartholomeus HM, Clevers JG, Behzad M (2013) Estimating salinity stress in sugarcane fields with spaceborne hyperspectral vegetation indices. *Int J Appl Earth Obs Geoinform* 21:282–290
- Haryani NS, Sulma S, Pasaribu JM (2017) Detection of acid sludge contaminated area based on Normalized Difference Vegetation Index (NDVI) value. *Int J Remote Sens Earth Sci* 11(1):21–32

- Haseena HK, Kiran BR, Shankar MK (2013) Application of aerial photography & remote sensing in environmental and geological interpretations in India-An Overview. *Int J Environ Biol* 3 (3):100–114
- Holm A, Cridland S, Roderick M (2003) The use of time-integrated NOAA NDVI data and rainfall to assess landscape degradation in the arid shrub land of Western Australia. *Remote Sens Environ* 85(2):145–158
- Huete AR (1998) A soil-adjusted vegetation index (SAVI). *Remote Sens Environ* 25:295–309
- Huete A, Miura T, Gao X (2003) Land cover conversion and degradation analyses through coupled soil–plant biophysical parameters derived from Hyperspectral EO-1 Hyperion. *IEEE Trans Geosci Remote Sens* 41:1268–1276
- IPES-Food (2019) From uniformity to diversity: a paradigm shift from industrial agriculture to diversified agro-ecological systems. International Panel of Experts on Sustainable Food Systems. <http://www.ipes-food.org/img/upload/files/UniformityToDiversityFULL>
- Islam MR, Abdullah HM, Ahmed ZU, Islam I, Ferdush J, Miah MG, Miah MM (2018) Monitoring the spatiotemporal dynamics of waterlogged area in southwestern Bangladesh using time series Landsat imagery. *Remote Sens Appl Soc Environ* 9:52–59
- Jabbar MT, Chen X (2008) Land degradation due to salinization in arid and semi-arid regions with the aid of geo-information techniques. *Geo-Spatial Inform Sci* 11(2):112–120
- Jain R (2011) Feasibility study on potential use of microwave SAR data in soil salinity induced land degradation assessment. M.Tech thesis, Andhra University, pp 1–97
- Jayawickreme DH, Van Dam RL, Hyndman DW (2008) Subsurface imaging of vegetation, climate, and root-zone moisture interactions. *Geophys Res Lett* 35(18)
- Jha MK, Chowdhury A, Chowdary VM, Peiffer S (2007) Groundwater management and development by integrated remote sensing and geographic information systems: prospects and constraints. *Water Resour Manag* 21(2):427–467
- Kaushik S, Dhote PR, Thakur PK, Aggarwal SP (2018) Assessing the impact of canal network on surface waterlogging using remote sensing datasets in Rohtak district, Haryana. *Int Arch Photogramm Remote Sens Spatial Inform Sci XLII-5:261–266*
- Kemna A, Vanderborght J, Kulesa B, Vereecken H (2002) Imaging and characterisation of subsurface solute transport using electrical resistivity tomography (ERT) and equivalent transport models. *J Hydrol* 267:125–146
- Khan NM, Rastoskuev VV, Sato Y, Shiozawa S (2005) Assessment of hydrosaline land degradation by using a simple approach of remote sensing indicators. *Agric Water Manag* 77:96–109
- Kniivila M (2004) Land degradation and land use/cover data sources. Working Document. United Nations: Department of Economic and Social Affairs, Statistics Division
- Koganti T, Najary B, Pathan A, Huang J, Triantafilis J (2018) Quantitative mapping of soil salinity using the DUALEM -21S instrument and EM inversion software. *Land Degrad Dev* 29:1768–1781
- Kumar S, Ghosh G, Saha SK (2015) Hyperspectral remote sensing data derived spectral indices in characterizing salt-affected soils: a case study of Indo-Gangetic plains of India. *Environ Earth Sci* 73(7):3229–3308
- Kwarteng AY (2002) Utilization of remote sensing and GIS for groundwater exploration. In: Singh S, Al-Rashed M (eds) *Kuwait Sherif. Groundwater hydrology*, Balkema, pp 157–178
- Lal R (2011) Soil carbon sequestration. SOLAW background thematic report- TR04B, Food and Agriculture Organization of the United Nations, Rome, p 36
- Lal R, Stewart BA (1990) Soil degradation: a global threat. *Adv Soil Sci* 11:XIII–XVIII
- Lambin EF, Meyfroidt P (2011) Global land use change, economic globalization, and the looming land scarcity. *Proc Natl Acad Sci* 108(9):3465–3472
- Lambin EF, Gibbs HK, Ferreira L, Grau R, Mayaux P, Meyfroidt P, Morton DC, Rudel TK, Gasparri I, Munger J (2013) Estimating the world's potentially available cropland using a bottom-up approach. *Glob Environ Chang* 23(5):892–901
- Lamble P, Fraser D (2002) Creation of a GIS-based predictive model for groundwater in the Murray Valley irrigation region (NSW). *Cartography* 31(1):33–44

- Lasne Y, Paillou P, Ruffie G, Serradilla C, Demontoux F, Freeman A, Farr T, McDonald K, Chapman B, Malezieu X (2008) Effect of salinity on the dielectric properties of geological materials: implication for soil moisture detection by means of remote sensing. *IEEE Trans Geosci Remote Sens* 46(6):1674–1688
- Leone AP, Sommer S (2000) Multivariate analysis of laboratory spectra for the assessment of soil development and soil degradation in the Southern Apennine (Italy). *Remote Sens Environ* 72:346–359
- Lu N, Zhang Z, Gao Y (2005) Recognition and mapping of soil salinization in arid environment with hyperspectral data. *Proc. IGARSS 2005. IEEE Int* 6:4520–4523
- Ludwig R, Gerhards H, Klenk, P, Wollschläger U, Buchner J (2011) Electromagnetic methods in applied geophysics. Institute of Environmental Physics, Heidelberg University, p 1–59
- Mandal AK (2019) Modern technologies for diagnosis and prognosis of salt-affected soils and poor-quality waters. In: Dagar J, Yadav R, Sharma P (eds) *Research Developments in Saline Agriculture*. Springer, Singapore, pp 95–152
- Mandal AK, Sharma RC, Singh G, Dagar JC (2010) Computerized database on salt affected soils in India. *Technical Bull./2/2010. CSSRI, Karnal*, p 28
- Mandal AK, Sethi M, Yaduvanshi NPS, Yadav RK, Bundela DS, Chaudhari SK, Anil C, Sharma DK (2013) Salt affected soils of Nain experimental farm: site characteristics, reclaimability & potential use. *Tech Bull, CSSRI, Karnal* 03:34
- Meena RS, Mitran T, Kumar S, Yadav G, Bohra JS, Datta R (2018) Application of remote sensing for sustainable agriculture and forest management. *Informat Proc Agric* 5:295–297
- Melendez-Pastor I, Navarro-Pedreño J, Koch M, Gómez I (2010) Applying imaging spectroscopy techniques to map saline soils with ASTER images. *Geoderma* 158:55–65
- Metternicht GI (1998) Fuzzy classification of JERS-1 SAR data: an evaluation of its performance for soil salinity mapping. *Ecol Model* 111:61–74
- Metternicht GI, Zinck JA (2003) Remote sensing of soil salinity: potentials and constraints. *Remote Sens Environ* 85:1–20
- Metternicht GI, Zinck JA (eds) (2008) *Remote sensing of soil salinization: impact on land management*. CRC Press, Taylor & Francis, Boca Raton, p 377
- Mitran T, Ravisankar T, Fyze MA, Suresh JR, Sujatha G, Sreenivas K (2015) Retrieval of soil physicochemical properties towards assessing salt-affected soils using Hyperspectral Data. *Geocarto Int* 30(6):701–721
- Mitran T, Lal R, Mishra U, Meena RS, Ravisankar T, Sreenivas K (2018) Climate change impact on soil carbon stocks in India. In: Lal R, Stewart BA (eds) *Advances in soil science, Soil and climate*, pp 291–308
- NAAS (2017) *Mitigating land degradation due to water erosion*. Policy Paper No. 88 National Academy of Agricultural Sciences, New Delhi, p 20
- Narjary B, Jangra P, Abhishek R, Kumar N, Raju R, Thimappa K, Meena RL, Kumar S, Kumar P, Chichmatalpure AR, Kamra SK (2017) Quantitative assessment of soil salinity using electromagnetic induction technique and geostatistical approach. *J Soil Salin Water Qual* 9:156–166
- Narjary B, Meena MD, Kumar S, Kamra SK, Sharma DK, Triantafilis J (2019) Digital mapping of soil salinity at various depths using an EM38. *Soil Use Manag* 35:232–244
- NBSS&LUP (2006) *Soils of India*. NBSS Pub. 94. National Bureau of Soil Survey and Land Use Planning, Nagpur, India
- NRSC (2010) *Wasteland Atlas of India*. National Remote Sensing Centre, ISRO, Hyderabad, p 140
- NRSC (2015) *Land degradation Atlas of India*. National Remote Sensing Centre, ISRO, Hyderabad
- NRSC (2020) *Land degradation Atlas of India*. National Remote Sensing Centre, ISRO, Hyderabad
- Odeh IO, Onus A (2008) Spatial analysis of soil salinity and soil structural stability in a semiarid region of New South Wales, Australia. *Environ Manag* 42(2):265
- Oldeman LR, Hakkeling RTA, Sombroek WG (1991) World map of the status of human-induced soil degradation: An explanatory note (GLASOD project). ISRIC, Wageningen, the Netherlands and UNEP, Nairobi, Kenya
- Oldeman LR (1992) Global extent of soil degradation. In: *Bi-Annual Report 1991–1992*. ISRIC, Wageningen, pp 19–36

- Periasamy S, Shanmugam RS (2017) Multispectral and microwave remote sensing models to survey soil moisture and salinity. *Land Degrad Dev* 28(4):1412–1425
- Rai AK, Basak N, Sundha P (2020) Chemistry of salt-affected soils. In: Minhas PS et al (eds) *Salinity management in India*. Central Soil Salinity Research Institute, Karnal, Haryana. (Submitted to ICAR, New Delhi)
- Rao BRM, Ravisankar T, Dwivedi RS, Thammappa SS, Venkataratnam L, Sharma RC, Das SN (1995) Spectral behaviour of salt-affected soils. *Int J Remote Sens* 16:2125–2136
- Ravishankar T, Sreenivas K (2010) Soils and land degradation. In: Roy PS, Dwivedi RS, Vijayan D (eds) *Remote sensing applications*. NRSC, ISRO, Hyderabad, pp 81–107
- Rawat KS, Mishra SV, Singh SK (2018) Integration of earth observation data and spatial approach to delineate and manage Aeolian Sand-Affected Wasteland in Highly Productive Lands of Haryana, India. *Int J Geoph* 1–7 <https://doi.org/10.1155/2018/2847504>
- Reddy VR (2003) Land degradation in India extent, costs and determinants. *Econ Polit Wkly* 38 (44):4700–4713
- Reiche J, Verbesselt J, Hoekman D, Herold M (2015) Fusing Landsat and SAR time series to detect deforestation in the tropics. *Remote Sens Environ* 156:276–293
- Robinson DA, Jones SB, Wraith JM, Or D, Friedman SP (2003) A review of advances in dielectric and electrical conductivity measurements in soils using time domain reflectometry. *Vadose Zone J* 2:444–475
- Saadoud D, Hassani M, Peinado FJ, Guettouche MS (2018) Application of fuzzy logic approach for wind erosion hazard mapping in Laghouat region (Algeria) using remote sensing and GIS. *Aeolian Res* 32:24–34
- SAC (2016) *Desertification and land degradation Atlas of India (Based on IRS AWiFS data of 2011–13 and 2003–05)*. Space Applications Centre, ISRO, Ahmedabad, p 219
- Sakala E, Fourie F, Gomo M, Coetzee H (2017) Mapping surface sources of acid mine drainage using remote sensing: case study of the Witbank, Ermelo and Highveld coalfields. *Mine Water and Circular Economy*, Lappeenranta, pp 1246–1253
- Samra JS, Sharma UC, Dadhwal KS (2012) Soil erosion and soil conservation. In: Goswami NN et al (eds) *Fundamentals of soil science*, p 725
- Sander P (2007) Lineaments in groundwater exploration: a review of applications and limitations. *Hydrogeol J* 15(1):71–74
- Saxena RK, Srivastava R Verma KS (2005) Spectral library of Indian Soils. *Tech. Bull. No. 5*, NATP, National Bureau of Soil Survey and Land Use Planning, Nagpur, India
- Sethi M, Dasog GS, Van Lieshout A, Salimath SB (2006) Salinity appraisal using IRS images in Shorapur Taluka, Upper Krishna Irrigation Project-Phase I, Gulbarga District, Karnataka, India. *Int J Remote Sens* 27:2917–2926
- Sethi M, Bundela D, Yadav RK, Manjit S (2014) Development of Spectral Reflectance Methods and Low Cost Sensors for Real-Time Application of Variable Rate Inputs in Precision Farming, Component 4 of NAIP, NAIP, ICAR Final Report
- Setia R, Lewis M, Marschner P, Raja Segaran R, Summers D, Chittleborough D (2013) Severity of salinity accurately detected and classified on a paddock scale with high resolution multispectral satellite imagery. *Land Degrad Dev* 24(4):375–384
- Sharda VN, Dogra P, Prakash C (2010) Assessment of production losses due to water erosion in rainfed areas of India. *J Soil Water Conserv* 65(2):79–91
- Shepherd KD, Walsh MG (2002) Development of reflectance spectral libraries for characterization of soil properties. *Soil Sci Soc Am J* 66:988–998
- Singh G, Bundela DS, Sethi M, Lal K, Kamra SK (2010) Remote sensing and GIS for appraisal of salt-affected soils in India. *J Environ Qual* 39(1):5–15
- Slater LD, Sandberg SK (2000) Resistivity and induced polarization monitoring of salt transport under natural hydraulic gradients. *Geophysics* 65:408–420
- Sreenivas K, Venkataratnam L, Narasimha Rao PV (1995) Dielectric properties of salt-affected soils. *Int J Remote Sens* 16:641–649
- Srivastava R, Sethi M, Yadav RK, Bundela DS, Singh M, Chattaraj S, Singh SK, Nasre RA, Bishnoi SR, Dhale S, Mohekar DS, Barthwal AK (2017) Visible-Near Infrared Reflectance

- Spectroscopy for Rapid Characterization of Salt-Affected Soil in the Indo-Gangetic Plains of Haryana, India. *J Indian Soc Remote Sens* 45(2):307–315
- Sterk G (2003) Causes, consequences and control of wind Erosion in Sahelian Africa: a review. *Land Degrad Develop* 14:95–108
- Stevens A, Nocita M, Toth G, Montanarella L, van Wesemael B (2013) Prediction of soil organic carbon at the European scale by visible and near infra red reflectance spectroscopy. *PLoS One* 8: e66409
- Taylor G, Dehaan R (2000) Salinity mapping with hyperspectral imagery. In: 14th International conference, Applied Geologic Remote Sensing, Springer, Netherlands, Las Vegas, pp 512–519
- Teng H, Rossel RA, Shi Z, Behrens T, Chappell A, Bui E (2016) Assimilating satellite imagery and visible–near infrared spectroscopy to model and map soil loss by water erosion in Australia. *Environ Model Softw* 77:156–167
- Tilley DR, Ahmed M, Son JH, Badrinarayanan H (2007) Hyperspectral reflectance response of freshwater macrophytes to salinity in a brackish subtropical marsh. *J Environ Qual* 36:780–789
- Tyagi NK (1998) Improvement of irrigation system for control of salinity. In: Tyagi NK, Minhas PS (eds) *Agricultural salinity management in India*. ICAR-CSSRI, Karnal, pp 309–324
- UNCCD (2017) *Global land outlook*. Germany, pp. 336
- UNEP (1992) *World Atlas of desertification*. London, Edward Arnold, p 69
- Viscarra Rossel R, Webster R (2012) Predicting soil properties from the Australian soil visible-near infrared spectroscopic database. *Eur J Soil Sci* 63:848–860
- Viscarra Rossel R, Behrens T, Ben-Dor E, Brown DJ, Demattê JA, Shepherd KD, Shi Z, Stenberg B, Stevens A, Adamchuk V, Aïchi H (2016) A global spectral library to characterize the world's soil. *Earth Sci Rev* 155:198–230
- Wang Q, Li P, Chen X (2012) Modeling salinity effects on soil reflectance under various moisture conditions and its inverse application: a laboratory experiment. *Geoderma* 170:103–111
- Weiss E, Marsh SE, Pfirman ES (2001) Application of NOAA-AVHRR NDVI time-series data to assess changes in Saudi Arabia's Rangelands. *Int J Remote Sens* 22(6):1005–1027
- Weng Y, Gong P, Zhu Z (2008) Soil salt content estimation in the Yellow River Delta with satellite hyperspectral data. *Canadian J Remote Sens* 34(3):259–270
- Wu CY, Jacobson AR, Laba M, Kim B, Baveye PC (2010) Surrogate correlations and near-infrared diffuse reflectance sensing of trace metal content in soils. *Water Air Soil Pollut* 209 (1–4):377–390
- Yan H, Wang S, Wang C, Zhang G, Patel N (2005) Losses of soil organic carbon under wind erosion in China. *Glob Chang Biol* 11:828–840
- Zhou Y, Guo B, Wang S, Tao H (2015) An estimation method of soil wind erosion in Inner Mongolia of China based on geographic information system and remote sensing. *J Arid Land* 7 (3):304–317